Journal of Applied Polymer Science

Carbon nanotubes/chitin nanowhiskers aerogel achieved by quaternization-induced gelation

Ignacio Garcia,[1] Itxaso Azcune,[1] Pablo Casuso,[1] Pedro M. Carrasco,[1] Hans-J. Grande,[1] Germán Cabañero,[1] Dimitrios Katsigiannopoulos,[2]* Eftychia Grana,[2] Konstantinos Dimos,[2] Michael A. Karakassides,[2] Ibon Odriozola,[1] Apostolos Avgeropoulos[2]

Materials Division, IK4-CIDETEC Research Center, Parque Tecnológico de San Sebastián, 20009 Donostia-San Sebastián, Spain
Department of Materials Science Engineering, University of Ioannina, University Campus—Dourouti, Ioannina 45110, Greece
*Present address: Université de Bordeaux, CNRS, Laboratoire de Chimie des Polymères Organiques (LCPO), UMR 5629, IPB-ENSCBP, 16 avenue Pey-Berland, 33607 Pessac Cedex, France.
Correspondence to: I. Garcia (E-mail: iggarcia@cidetec.es)

ABSTRACT: Organic aerogels from polysaccharides such as cellulose and chitin are of particular importance because they utilize renewable feedstocks. In this article, the aerogels were prepared through the self-assembly of chitin nanowhiskers previously modified. The surface of chitin nanowhiskers was rendered cationic through two reactions. A first reaction between hydroxyl groups of chitin and 2-chloroethyl isocyanate and a second reaction between the chloride groups of isocyanate anchored to the surface and 1-methylimidazole. This modification led to stable aqueous suspensions of the chitin nanowhiskers with gelation and rheological properties. Additionally, chitin nanowhiskers aerogels containing modified carbon nanotubes were obtained. The addition of modified carbon nanotubes provoked a change in the morphology of the hydrogels and as a consequence, the rheological properties of the hydrogel are modified as well. In contrast from previous procedures, this method has not required any kind of solvent exchange or high pressure in order to obtain the final materials. © 2015 Wiley Periodicals, Inc. J. Appl. Polym. Sci. **2015**, *132*, 42547.

KEYWORDS: biomaterials; biopolymers & renewable polymers; polysaccharides

Received 14 January 2015; accepted 26 May 2015
DOI: 10.1002/app.42547

INTRODUCTION

Chitin is the second most abundant natural polymer after cellulose.[1] Chitin, consisting of β (1–4) linked 2-acetamido-2-deoxy-D-glucose units, is mainly synthesized via a biosynthetic manner by an enormous number of living organisms, such as shrimps, crabs, tortoises, and insects.[1] Even if it can also be synthesized by a non-biosynthetic pathway through chitinase-catalyzed polymerization of a chitobiose oxazoline derivatives, crab and shrimp shells are the most common source of chitin. Analogous to cellulose, chitin consists of both crystalline and amorphous domains. The amorphous domains can be hydrolyzed to release the crystalline segments, so-called chitin nanowhiskers, by using an acid hydrolysis procedure.[2] Despite its huge annual production and easy accessibility, chitin still remains an unutilized biomass resource primarily due to its intractable bulk structure and insolubility in aqueous and organic media.[3] Therefore, the potential applications of chitin have not been fully exploited yet, and remain as an active field of research.

Chemical modification of chitin, as well as of other polysaccharides, is one of the most efficient approaches to explore their potential, giving rise to novel types of functional materials. Many researchers have been focusing on the preparation of chitin derivatives. Chitin possesses a reactive surface covered with hydroxyl and acetamide groups, which enables direct modification through chemical reactions. Various chemical transformations as N-deacetylation, acetylation, and others have been used to make chitin more easily dispersible in a given medium while increasing the scope of its applications.[4–8] Quaternization is one of the various methods that can enhance water dispersion. Quaternized chitin can find its application in environmental, food, and biomedical fields.

On the other hand, aerogels are unique materials that display unusual and highly desirable properties such as low densities, high porosities, high internal surface areas, and low heat conductivity.[9] As a result, aerogels find application in areas such as catalysis, thermal insulation, drug delivery, gas storage, liquid absorption, and space and particle research.[10–13] Organic aerogels, specifically aerogels made from polysaccharides such as cellulose and chitin, are of particular importance since they utilize renewable feedstocks. Previously, chitin aerogels have been

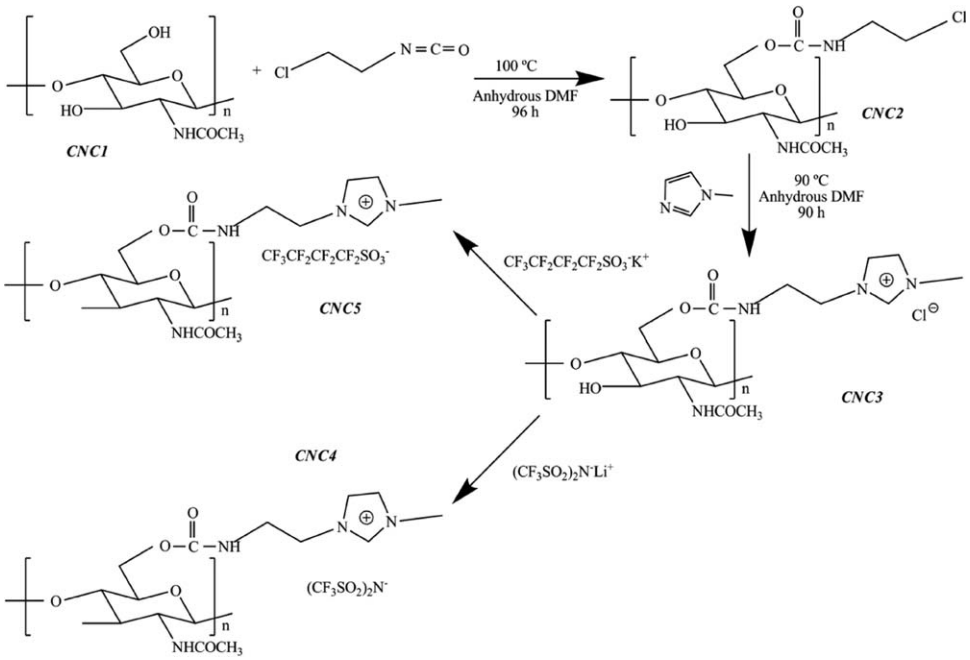

Figure 1. Synthesis and anion-exchange of ionic chitin nanowhiskers.

prepared by using the dissolution of chitin followed by regeneration in solvent, typically ethanol. Chitin dissolution systems include *N*,*N*-dimethylacetamide/lithium chloride, 1-butyl-3-imidazolium acetate, and NaOH–urea solutions.[14–16] In a different approach, Nogi *et al.* reported a chitin aerogel made from chitin nanofibers by using a freeze-drying technique.[17] Recently, Heath *et al.* were the first group reporting chitin nanowhiskers aerogel.[18] in this research work, the chitin nanowhiskers were sonicated in water to form a hydrogel prior to solvent exchange with ethanol and drying under supercritical CO_2.

In the work presented in this manuscript, we report the preparation of chitin nanowhiskers aerogels and chitin nanowhiskers hybrids aerogels containing carbon nanotubes via chemical modification of chitin nanowhiskers with imidazolium moieties. The method described has not required any kind of solvent exchange or critical conditions in contrast to what has been reported in the literature. The two-step functionalization of chitin led to an ionic material that forms stable hydrogels. Once formed, the hydrogels were plunged into liquid nitrogen until freeze dried leading to the formation of an aerogel. The addition of modified carbon nanotubes provoked a change in the morphology of the hydrogels and as a consequence, a decrease of their storage and loss modulus was evident.

EXPERIMENTAL

Materials

Chitin from shrimp shells-practical grade, 2-chloroethyl isocyanate-97% (CEI) and 1-methylimidazole-99% (MIZ), anhydrous *N*,*N*-dimethylformamide (DMF) bis(trifluoromethylsulfonyl)-imine lithium salt (LiTFSi), and nonafluoro-1-butanesulfonic acid potassium (KNONA) salt were purchased from Sigma-Aldrich and used as received. Tetrahydrofuran-synthesis grade (THF), hydrochloride acid (HCl), and ethyl acetate-synthesis grade were obtained from Scharlau and were used as received.

Isolation of Chitin Nanowhiskers

Commercial chitin was hydrolyzed in 3*M* HCl for 1.5 h at 90°C to digest the disordered regions. After this process, the chitin was recovered by centrifugation and resuspended in distilled water in order to reduce the acid concentration. This chitin suspension was then diluted against several changes of distilled water until pH = 6 was reached.[19] Afterwards, chitin nanowhiskers were freeze-dried (denoted as CNC1 in the rest of the manuscript).

Synthesis of Ionic Chitin Nanowhiskers

In this part of the manuscript, the synthesis of ionic chitin nanowhiskers is described. Figure 1 shows a schematic representation for the synthesis of ionic chitin nanowhiskers, involving as well the anion-exchange that was carried out in order to modify the chitin dispersion. Ionic chitin nanowhiskers were prepared following the procedure described in the literature.[20–22]

One suspension of freeze-dried chitin nanowhiskers in DMF was sonicated for 5 min and introduced into a two-neck flask equipped with a magnetic stirring bar under continuous nitrogen flow. Then, the flask was immersed in an oil bath and heated up to 100°C. The required volume of CEI was added to the reaction flask and the functionalization was carried out for 96 h. Chemical modification was performed in CNC/CEI molar ratios equal to 1 : 5, which led to 2-chloroethylisocyanate-containing chitin nanowhiskers denoted as CNC2 in the rest of the manuscript. Modified chitin nanowhiskers were recovered after removal of the non-grafted CEI with THF by means of a solubilization-centrifugation technique. This process was repeated at least three times, in order to remove any unreactive

CEI. The CNC2 were then dried under vacuum at 40°C for a period of 2 days.

One suspension of dried CNC2 in DMF was sonicated for 5 min and introduced into a two-necked flask equipped with a magnetic stirring bar under nitrogen flow. Then, the flask was immersed in an oil bath and heated up to 90°C. The required volume of MIZ was added to the reaction flask and functionalization was carried out for 96 h. Chemical modification was performed in CNC2/MIZ weight ratios equal to 1 : 4, which led to 1-methylimidazole-containing chitin nanowhiskers denoted as CNC3 from herein. The modified chitin nanowhiskers were then subsequently washed with ethyl acetate and dried under vacuum at 40°C for a period of 2 days.

Procedure for the Anion-Exchange Method

To prepare ionic chitin nanowhiskers having bis(trifluoromethylsulfonyl)imine (denoted as CNC4 in the rest of the manuscript) or nonafluoro-1-butanesulfonic acid (denoted as CNC5) as anions, a very diluted solution of LiTFSI or KNONA in distilled water and a dispersion of 0.5 g of CNC3 in 50 mL of distilled water were mixed together in a round-bottom flask. After 30 min of stirring at room temperature, the resulting CNC4 or CNC5 species were obtained in the form of precipitates. Modified chitin nanowhiskers were recovered, after removal of the excess of salt with water, by means of a solubilization-centrifugation technique and were finally freeze-dried.

Synthesis of Composites Material Based on Carbon Nanotubes

Modified carbon nanotubes were made following our previous article.[23] In this article, we reported the synthesis of a composite material comprised of poly(4-vinylpyridine) (P4VP) grafted on multiwall carbon nanotubes (CNT) and the preparation of a nanohybrid via quaternization of the nitrogen atom per monomeric unit of the polymer chains. 4-Vinylpyridine was polymerized anionically using high vacuum techniques and was reacted with CNTs under vacuum to be grafted on the polymer segments. The dispersion of the carbon nanotubes was improved after quaternization due to the formation of CNT-*g*-[P42VP-*r*-poly(4-vinylpyridinium bromide)] (CNT-*g*-[P4VP-*r*-poly(4ViEt-Py^+Br^-)]).

Hydrogel Preparation

Modified freeze-dried chitin nanowhiskers were used to produce the hydrogel and subsequently obtain the corresponding aerogel. Hydrogels were produced by dispersing 0.058 g of modified nanowhiskers in 1 mL deionized water at room temperature using a sonicator for 5 min at maximum power, with a maximum temperature of 30°C. Afterwards, the dispersions were left at ambient conditions, for complete water evaporation. The point of gelation was determined as the point at which the vial could be inverted without net movement of the gel.

Hybrid Hydrogel Preparation

Similar procedure to that for the preparation of neat hydrogels was used in order to obtain the hybrid hydrogels. CNC3 chitin nanowhiskers were added into an aqueous dispersion of CNT-*g*-[P4VP-*r*-poly(4ViEt-Py^+Br^-)] (varied at 2 and 10 wt % with respect to the weight of chitin nanowhiskers) and sonicated for 5 min at maximum power, with a maximum temperature of 30°C. Subsequently, the dispersions were again left at ambient conditions, for water evaporation. The point of gelation was determined as the point at which the vial could be inverted without net movement of the gel.

Chitin Aerogel Preparation

Once formed, the hydrogels were plunged into liquid nitrogen to freeze prior to being attached to a Heto PowerDry LL3000 freeze dryer until the aerogel was obtained.

Techniques

Nuclear magnetic resonance (NMR) spectra were obtained using a Bruker 400 WB Plus spectrometer. Spectra were collected using a 4 mm cross polarization magic-angle spinning (CP-MAS) probe at a spinning rate of 6000 Hz. CP-MAS ^{13}C spectra of solid samples were recorded for 12 h using the standard pulse sequence, at 100.6 MHZ, a time domain of 2 K, a spectral width of 29 kHz, a contact time of 1.5 ms, and an interpulse delay of 5 s for ^{13}C, a time domain of 1 K, a spectral width of 55 kHz, a contact time of 2 ms.

Fourier transform infrared (FTIR) spectroscopy was recorded at room temperature on a Nicolet Avatar 360 spectrophotometer. The spectra were taken with a 4 cm^{-1} resolution in a wavenumber range from 4000 to 400 cm^{-1}.

Elemental analysis was performed using a LECO Micro Truspec CHN to measure carbon, nitrogen, and hydrogen contents independently.

Atomic force microscopy (AFM) images of the samples were obtained in tapping mode at room temperature using a scanning probe microscope (Molecular Imagings PicoScan) equipped with a Nanosensors tips/cantilever, a resonance frequency of ~330 kHz, and a spring constant of ~42 N/m with a tip nominal radius lower than 7 nm.

Thermal gravimetric analysis (TGA) measurements were carried out with a TA-Instrument Q500 TGA using a temperature range of 30–600°C at a heating rate of 10°C min^{-1} under nitrogen. Typical sample weight was approximately equal to 5 mg for all experiments.

X-ray diffraction patters of the chitin nanowhiskers were collected using the spectrometer X'Pert MPD by "Philips" with Cu Kα radiation (the wavelength is $\lambda = 1.54056$ Å).

The micromorphology of the hydrogel samples was evaluated using a field emission scanning electron microscopy. The measurements were carried out in a Carl Zeiss Ultra Plus field emission scanning electron microscope equipped with an energy dispersive X-ray spectrometer (EDXS). The field emission scanning electron microscope (FE SEM) samples were prepared by freezing hydrogels in liquid nitrogen followed by lyophilization. The lyophilized samples were then coated with Au.

Dynamic rheology of the hydrogels was studied using a controlled stress/strain rheometer (Advanced Rheometer AR2000EX, TA Instruments) with a parallel plate. A neat hydrogel and two hydrogels containing carbon nanotubes were analyzed. The rheometer was cleaned prior to use with acetone and the temperature was maintained at 23°C with a double wall

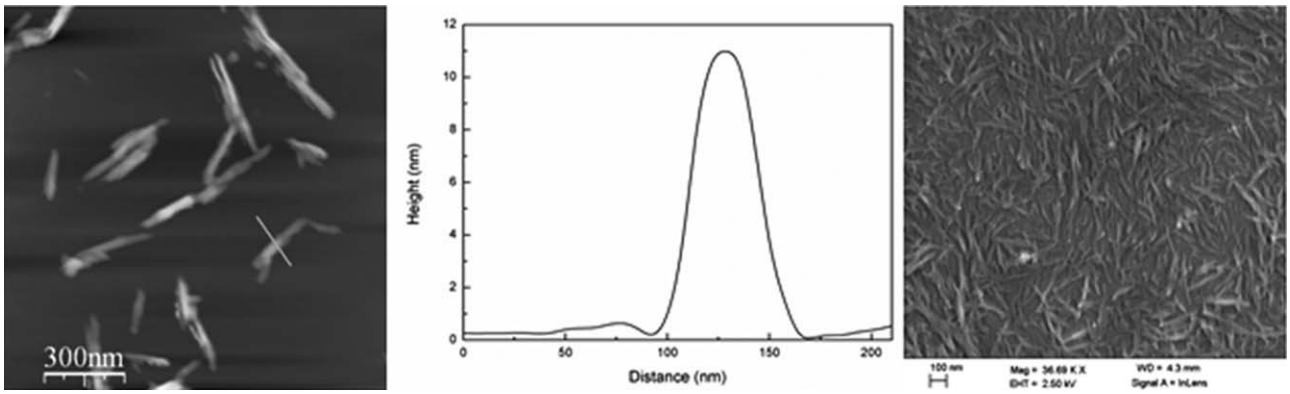

Figure 2. Height AFM image (left), corresponding height profile (center), and FE-SEM image of CNC1 sample (right).

Peltier bath. Oscillatory shear tests provided storage modulus (G'), and loss modulus (G'') which were plotted against angular frequency (ω). Before oscillatory frequency sweep measurements, the hydrogels were allowed to rest for 3–5 min. The sweeps were carried out between 0.7 and 100 Hz with controlled strain amplitudes of 1.

Mercury intrusion porosity measurements were performed with a Quantachrome PoreMaster-33 GT instrument. Pore size distributions were constructed according to the Washburn equation: $D = -(4\gamma\cos\vartheta)/P$, where D is the pore diameter expressed in μm, γ is the mercury surface tension (480 dyne/cm), ϑ is the contact angle between mercury and the pore wall (140°), and P is the applied pressure in psia.

RESULTS AND DISCUSSION

Chitin Nanowhiskers Characterization

After the acid hydrolysis treatment of chitin, dried powder was characterized by AFM and FE-SEM. Representative height AFM image and corresponding height profile as well as the FE-SEM image are shown in Figure 2 for sample CNC1. Samples were prepared through the water evaporation of very diluted dispersions of chitin on a mica surface. In the height profile, differences between the apparent CNC diameter and height can be observed. This fact can be attributed to the tip geometry smearing effect.[24] In general, the AFM tips have a finite size and shape. As the tip passes over a sample with the surface feature of comparable size as that of the tip, the shape of the tip eventually contributes to the formed image. The AFM images of CNC1 will therefore, in practice, be a convolution of the crystals and the tip geometry. This leads to a general broadening of the chitin crystals. An estimation of the thickness of the CNC1 was possible by measuring the difference of height between the mica surface and the chitin nanowhiskers. Acid hydrolysis of chitin led to rod-like chitin nanowhiskers whose high aspect ratio was estimated showing an average diameter of 10.3 ± 2.1 nm and a length of $\sim 248 \pm 31$ nm which was determined by line scans across several individual CNC1 samples. Figure 2 (right) shows a FE-SEM image of the hydrolyzed chitin suspension. The suspension contains chitin fragments consisting of both individual nanowhiskers and associated or collapsed nanowhiskers.

Modification of Chitin Nanowhiskers

Neat and modified chitin nanowhiskers were characterized by several techniques in order to corroborate the surface modification of chitin nanowhiskers. FTIR analysis was used further to observe the presence of any residual reactant in the modified nanowhiskers. FTIR of CNC1 (Figure 3) indicates that the material is pure chitin with split absorbance peaks corresponding to the amide I region at 1660 and 1620 cm^{-1} and an absorbance peak at 1560 cm^{-1} corresponding to the amide II region. After chemical treatment, the introduction of CEI was further confirmed in the CNC2 relative spectra by the appearance of new bands, like the ν-C═O stretching vibration at 1710 cm^{-1} in the amide I region corresponding to the urethane groups.[25] In addition, the absence of the peak at 2265 cm^{-1} corresponding to ─N═C═O groups, confirmed that, during the centrifuge steps, both CEI monomer in excess was removed completely and also, the isocyanate groups in CEI reacted with the hydroxyl groups of the corresponding chitin. The stretching bands corresponding to C═C and C═N at 1635 cm^{-1} and 1600 cm^{-1} respectively, are two peaks characteristic of imidazolium.[26] As can be observed in Figure 3, FTIR spectrum of CNC3 did not lead to different spectrum when it is compared

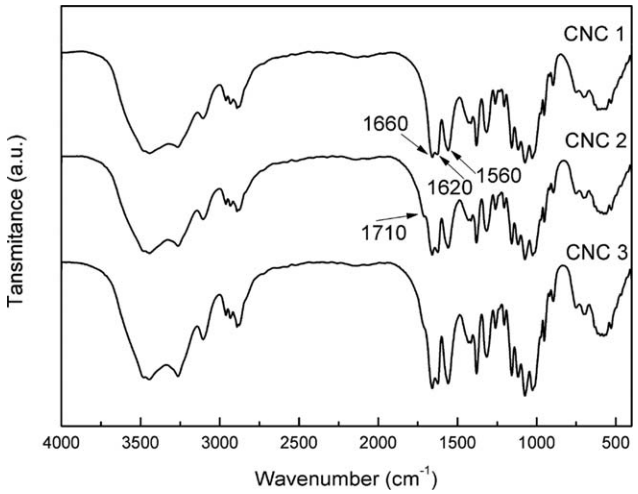

Figure 3. FTIR spectra of CNC1 and CNC2.

Table I. Elemental Weight Compositions for Unmodified and Modified CNC

Sample	N (wt %)	C (wt %)	H (wt %)
CNC1	5.99	35.59	6.36
CNC2	7.22	39.97	5.91
CNC3	7.81	39.57	6.16

with CNC1 and CNC2 spectra due to overlapping of the characteristic MIZ band with that of CNC2 and CNC1 respectively.

Additionally, elemental analysis of the samples was carried out to determine the grafted ratio of CEI and MIZ molecules per chitin monomeric unit. Results are listed in Table I. Grafting efficiency was calculated on the basis of nitrogen content, whose presence is indicative of the chemical addition of 1-methylimidazole. The grafting efficiency for CNC2 with chitin/isocyanate molar ratio 1 : 5 was found to be 0.1. Moreover, the grafting efficiency for CNC3 was 0.6 with respect to isocyanate molecules anchored to chitin.

In order to corroborate the surface modification of chitin nanowhiskers, ^{13}C-NMR characterization was also performed. The spectra obtained prior to and after chemical modification of chitin nanowhiskers are shown in Figure 4. The starting chitin nanowhiskers displayed typical peaks of chitin backbone at 23.2, 54.9, 60.3, 73.3, 76.1, 83.1, 104.0, and 172.1 ppm, which could be assigned to the carbons CH_3, C2, C6, C3, C5, C4, C1 and C═O respectively. As it can be observed in Figure 4, the appearance of a new peak in CNC2 and CNC3 at 173 ppm, corresponding to the carbonyl group of the urethane linkage, confirms the successful chemical modification of the chitin nanowhiskers.[27,28] Also, two new peaks at 43 and 37 ppm were assigned to the CH_2 bonded to the isocyanate group and to the CH_2 linked to the chloride atoms, respectively. Furthermore, the intensity increase of the peak at $\delta \approx 84$ ppm in CNC3 spectrum

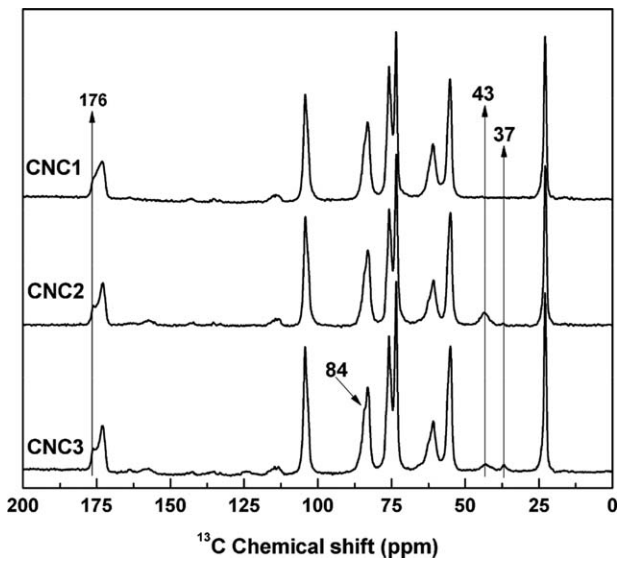

Figure 4. ^{13}C-NMR spectra of CNC1, CNC2, and CNC3 (top) and zoom areas where new peaks were observed (bottom).

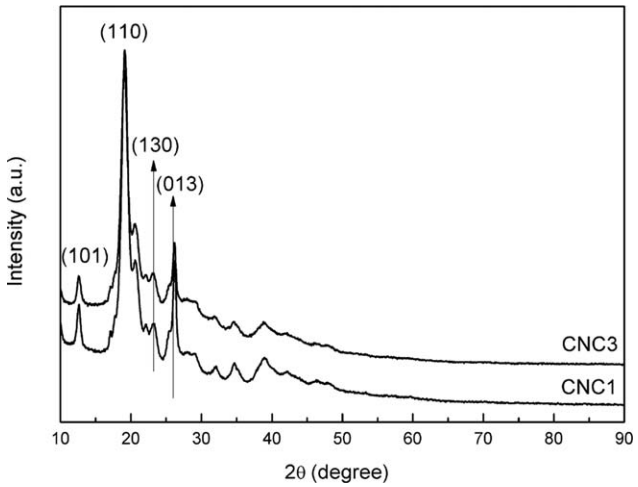

Figure 5. XRD patters of CNC1 and CNC3.

is attributed to carbons located between the two nitrogen atoms of imidazolium after quaternization. These observations eventually confirm the successful surface modification of the chitin nanowhiskers.

To obtain the crystalline degree of the samples, an X-ray study was carried out. Figure 5 shows the diffractograms of CNC1 and CNC3 respectively. Cárdenas *et al.* showed that the characteristic diffraction peaks of chitin were (101), (110), (130), and (013) at 12.58, 19.08, 23.22, and 25.99 degrees, respectively.[29] The crystalline index was determined according to the proposed method for cellulose. Therefore, by applying the method for cellulose to chitin the crystalline index of CNC1 and CNC3 samples was determined at 86.7 and 87.8 degrees, respectively. These values indicated that the surface modification of chitin did not affect the crystalline structure of the chitin nanowhiskers.

In order to study the thermal stability of neat and modified chitin nanowhiskers, TGA measurements were carried out. Figure 6 shows differential thermogravimetric curves (DTG) both of neat and modified chitin nanowhiskers. It was observed that the maximum degradation temperature of neat chitin nanowhiskers

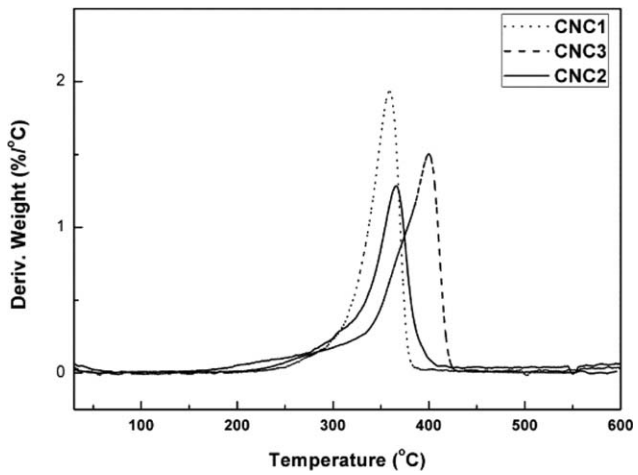

Figure 6. DTG curves of CNC1, CNC2, and CNC3.

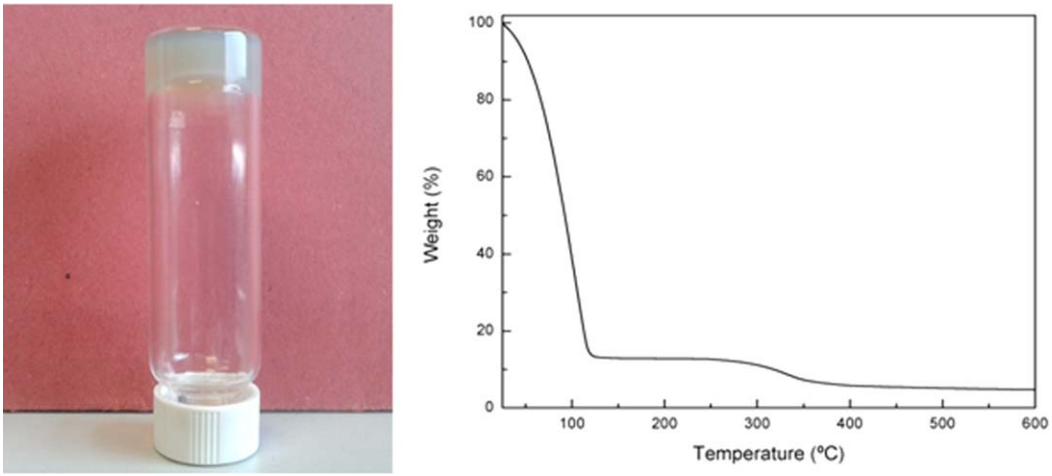

Figure 7. Photograph of the finally formed hydrogel obtained using CNC3 nanowhiskers (left) and corresponding TGA curve of the hydrogel containing CNC3 (right). [Color figure can be viewed in the online issue, which is available at wileyonlinelibrary.com.]

was 359°C. In the case of CNC2 and CNC3 samples, the maximum degradation temperature was 367 and 399°C, respectively. These degradation temperatures indicate that the surface modification of chitin nanowhiskers increases the thermal stability of chitin nanowhiskers.

Characterization of Chitin Nanowhiskers Hydrogels

As a general method, chitin nanowhiskers hydrogels were synthesized by the self-assembly of freeze-dried chitin nanowhiskers in deionized water at a concentration of 5.48 wt %. After sonication for 5 min, the fine dispersions were left at room temperature, for water evaporation. The point of gelation was determined as the point at which the vial could be inverted without net movement of the hydrogel. The dispersion containing CNC1 nanowhiskers did not form a gel, due to fast precipitation of the chitin nanowhiskers in water. On the other hand, the surface chemistry of the modified chitin nanowhiskers has been modified leading to the conclusion that interactions of the new substituents and changes in the surface structure have to be taken into account when investigating the gelation mechanism. The dispersion containing CNC2 showed the same behavior with that containing CNC1. In the case of dispersion containing CNC3, after 17 h an opaque hydrogel was obtained (Figure 7). In the same manner, several authors have shown that chloride salts anchored to cellulose nanowhiskers or carbon nanotubes enhance water uptake and their presence is likely to affect the behavior of the modified cellulose nanowhiskers or carbon nanotubes suspensions.[23,30] Comparable to studies already reported in the literature, dispersion in water of our chitin nanowhiskers is influenced by the imidazolium chloride salt anchored to the chitin nanowhiskers. This leads to enhanced hydrophylicity and better stability of the chitin nanowhiskers in water. The hydrogel was characterized by TGA in order to determine the final composition. Figure 7 (right) shows the TGA curve for CNC3 hydrogel. Two weight losses were observed. The first one, below 130°C, corresponds to evaporation of water in the hydrogel. The second one, between 250 and 400°C, is attributed to the degradation of chitin nanowhiskers. The percentage mass loss at 150°C is 85.96 wt %, therefore the content of chitin in the hydrogel is approximately higher than 10 wt %.

It is well-known that the nature of the anion influences the final properties of materials such as solubility, dispersion ability, viscosity, and thermal stability. Exchanging the chloride counterions with bis-trifluoromethane sulfonimide (CNC4) or nonafluoro-1-butanesulfonic acid counterions (CNC5) resulted in suspensions with remarkably different behavior. The ion-exchanged suspensions did not display tendency to gel in water. The dispersion containing CNC4 and CNC5 nanowhiskers did not form a gel, probably due to the fast precipitation of chitin nanowhiskers in water. This indicates that anionic groups on chitin nanowhiskers contribute to their dispersion ability and stability and the nature of the counterion is very likely an important factor in the formation of the final chitin nanowhiskers hydrogels.

The results of the oscillatory shear tests on CNC3 hydrogel and hybrids hydrogels are shown in Figure 8, where storage modulus (G'), and loss modulus (G'') are plotted against angular

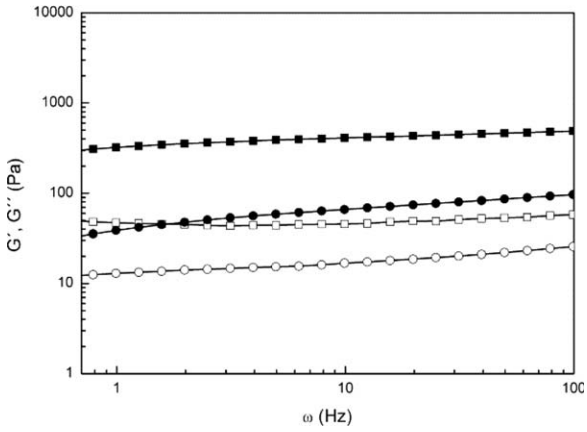

Figure 8. Oscillatory shear tests, storage modulus (G', closed symbols), and loss modulus (G'', opened symbols) as a function of angular frequency (ω) for neat CNC3 hydrogel (square) and CNC3 hydrogel with 2 wt % of CNT-*g*-[P4VP-*r*-poly(4ViEt-Py$^+$Br$^-$)] (circles).

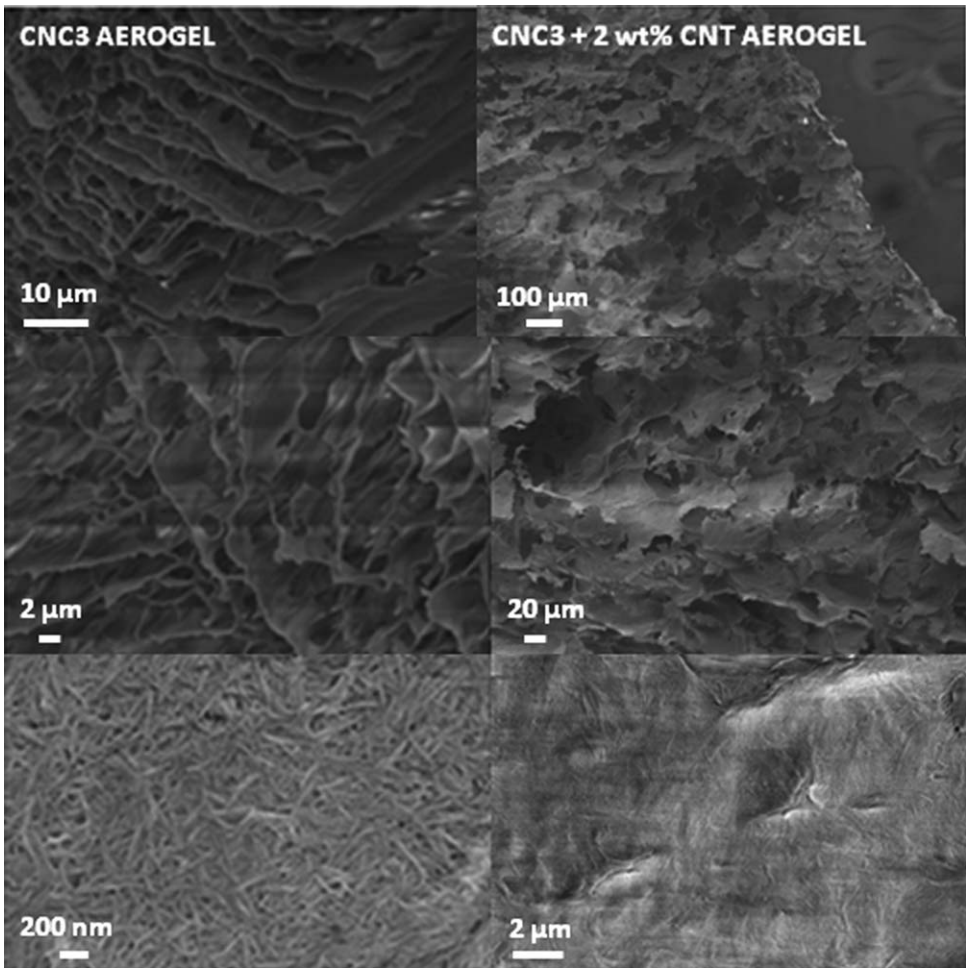

Figure 9. FE-SEM images of a representative chitin nanowhiskers aerogel (left) and hybrid aerogel (right) where the porous network and aggregation of chitin nanowhiskers are shown.

frequency (ω). In all cases a hydrogel was obtained, only with an exception at dispersion containing 10 wt % of CNT-*g*-[P4VP-*r*-poly(4ViEt-Py$^+$Br$^-$)]. In this case, the hydrogel was not formed. As general behavior, the storage modulus and loss modulus decrease when the quantity of CNT-*g*-[P4VP-*r*-poly(4-ViEt-Py$^+$Br$^-$)] was increased in the hydrogel. This confirms that the incorporation of CNT-*g*-[P4VP-*r*-poly(4ViEt-Py$^+$Br$^-$)] inhibits the formation of chitin hydrogel and leads to weak formation of hydrogels. For an ideal gel which behaves elastically, the modulus dependences are expected to be $G' \propto \omega^0$ and $G' >> G''$; the neat hydrogel most closely followed this relation, although, the hydrogels containing CNT-*g*-[P4VP-*r*-poly(4ViEt-Py$^+$Br$^-$)] showed larger deviations from the ideal hydrogel than from the neat hydrogel.

The aerogels were obtained from the corresponding hydrogels that were plunged into liquid nitrogen to freeze prior to being freeze dried until the aerogel was obtained. FE-SEM was used to image the internal porous network structure of the aerogel. FE-SEM micrographs of CNC3 aerogel are shown in Figure 9 (left) at three different magnifications. The aerogel sample exhibited well-ordered porous microstructures with aggregation of nanowhiskers in the form of interconnected sheets. The microstructures of hybrid hydrogels with content of 2 wt % of CNT-*g*-[P4VP-*r*-poly(4ViEt-Py$^+$Br$^-$)] is shown in Figure 9 (right). All hybrids hydrogels present a similar porous structure with aggregation of nanowhiskers and CNT-*g*-[P4VP-*r*-poly(4ViEt-Py$^+$Br$^-$)] in the form of flakes which are completely different to the structure observed for neat hydrogels. These results are in agreement with the rheological results. Probably, the decrease of storage and loss modulus of the hybrid hydrogels were provoked as a consequence of the structural change due to incorporation of CNT-*g*-[P4VP-*r*-poly(4ViEt-Py$^+$Br$^-$)] to the chitin nanowhiskers.

Mercury intrusion porosimetry was employed to reveal the porous character of the aerogels. The obtained pore size distribution curves for samples CNC3 aerogel, and CNC3 + 2 wt % CNT-*g*-[P4VP-*r*-poly(4ViEt-Py$^+$Br$^-$)] aerogel are shown in Figure 10. As observed, the CNC3 aerogel exhibits a dominant broad peak corresponding to pores with a diameter of 62 μm. In addition, CNC3 aerogel demonstrates a relatively narrow peak at 7.1 nm with no further contribution in the mesopores region. On the other hand, CNC3 + 2 wt % CNT-*g*-[P4VP-*r*-poly(4ViEt-Py$^+$Br$^-$)]aerogel displays a wide pore size distribution with variable pore diameters ranging from 4 to 300 μm and multiple maxima. Furthermore, two maxima are present in

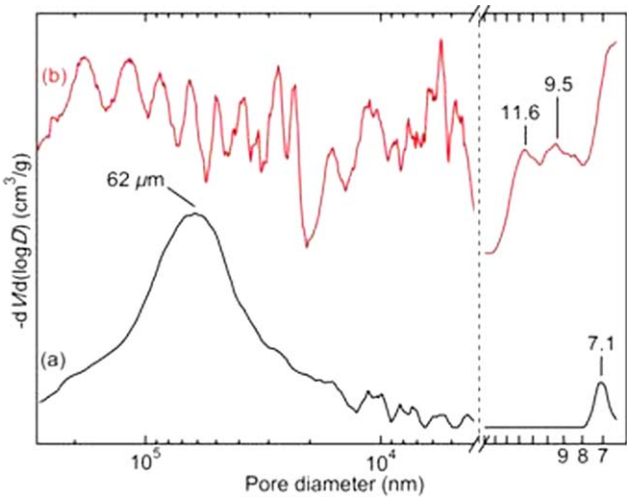

Figure 10. Pore size distributions obtained by mercury intrusion porosimetry for samples CNC3 aerogel (a), and CNC3 + 2 wt % CNT-*g*-[P4VP-*r*-poly(4ViEt-Py^{+}Br^{-})] aerogel (b). [Color figure can be viewed in the online issue, which is available at wileyonlinelibrary.com.]

the mesopores region at 11.6 and 9.5 nm. It should be taken into account that due to the pore filling mechanism, mercury porosimetry will always slightly underestimate pore sizes compared to FE-SEM observations and the calculated pore size by this technique.[31]

CONCLUSIONS

In the present study, mesoporous chitin nanowhisker aerogels were prepared by sonication-assisted assembly of modified chitin nanowhiskers in water to obtain a hydrogel followed by their plunging into liquid nitrogen to freeze-dry until the formation of an aerogel. This method has not required any kind of solvent exchange or high pressure to obtain the aerogels as reported in various techniques for corresponding materials reported in the literature. Chitin nanowhiskers with imidazolium moieties onto surface were synthesized by a two-step functionalization. The characterization results by FTIR, ^{13}C-NMR, and elemental analysis confirmed that the imidazolium groups have been anchored to the surface of the chitin nanowhiskers. XRD measurements confirmed that the surface modification of chitin nanowhiskers did not change the crystallinity of the native chitin.

Chitin nanowhiskers hydrogels behave elastically as ideal hydrogels. The addition of modified carbon nanotubes provoked a deviation from the ideal behavior, but a significant change in the morphology of hydrogels was evident and as consequence, a decrease of storage and loss modulus of the formed hydrogels was observed. These aerogels were prepared by using a simple process, which may allow new applications in a variety of areas such as thermal insulators, catalyst supports, and biomedical materials.

ACKNOWLEDGMENTS

The present work was supported by the European Projects ECLIPSE (NMP-280786) and PIL-to-MARKET (FP7-PEOPLE-IAPP-2008–230747).

AUTHOR CONTRIBUTIONS

Dr. Itxaso Azcune performed ^{13}C-NMR experiments. Dr. Pablo Casuso performed elemental analysis and rheological experiments. Dr. Pedro M. Carrasco performed FEM morphological characterization. Dr. Ignacio Garcia isolated and modified chitin nanowhiskers, performed AFM, TGA, and FTIR measurements, prepared chitin hydrogels and aerogels, supervised the research and wrote the manuscript. Dr. Apostolos Avgeropoulos supervised the research and wrote the manuscript. Dr. Konstantinos Dimos performed and Michael A. Karakassides supervised porosity experiments. Dimitrios Katsigiannopoulos and Eftychia Grana carried out the synthesis of composites material based on carbon nanotubes and their characterization. Hans-J. Grande and Germán Cabañero supervised the research and Ibon Odriozola supervised the manuscript.

REFERENCES

1. Kumar, M. N. V. R. *React. Funct. Polym.* **2000**, *46*, 1.
2. Zeng, J. B.; He, Y. S.; Li, S. L.; Wang, Y. Z. *Biomacromolecules* **2011**, *13*, 1.
3. Mine, S.; Izawa, H.; Kaneko, Y.; Kadokawa, J. I. *Carbohydr. Res.* **2009**, *344*, 2263.
4. Sashiwa, H.; Shigemasa, Y. *Carbohydr. Polym.* **1999**, *39*, 127.
5. Lamarque, G.; Chaussard, G.; Domard, A. *Biomacromolecules* **2007**, *8*, 1942.
6. Ifuku, S.; Morooka, S.; Morimoto, M.; Saimoto, H. *Biomacromolecules* **2010**, *11*, 1326.
7. Gopalan, N. K.; Dufresne, A. *Biomacromolecules* **2003**, *4*, 1835.
8. Pei, A.; Butchosa, N.; Berglund, L. A.; Zhou, Q. *Soft Matter* **2013**, *9*, 2047.
9. Kistler, S. S. *J. Phys. Chem.* **1932**, *36*, 52.
10. Moreno-Castilla, C.; Maldonado-Hodar, F. *J. Carbon* **2005**, *43*, 455.
11. Tsioptsias, C.; Stefopoulos, A.; Kokkinomalis, I.; Papadopoulou, L.; Panayiotou, C. *Green Chem.* **2008**, *10*, 965.
12. Mehling, T.; Smirnova, I.; Guenther, U.; Neubert, R. H. H. *J. Non-Cryst. Solids* **2009**, *355*, 2472.
13. Aaltonen, O.; Jauhiainen, O. *Carbohydr. Polym.* **2009**, *75*, 125.
14. Randall, J. P.; Meador, M. A. B.; Jana, S. C. *ACS Appl. Mater. Interfaces* **2011**, *3*, 613.
15. Tsioptsias, C.; Michailof, C.; Stauropoulos, G.; Panayiotou, C. *Carbohydr. Polym.* **2009**, *76*, 535.
16. Ding, B. B.; Cai, J.; Huang, J. C.; Zhang, L. N.; Chen, Y.; Shi, X. W.; Du, Y. M.; Kuga, S. *J. Mater. Chem.* **2012**, *22*, 5801.
17. Nogi, M.; Kurosaki, F.; Yano, H.; Takano, M. *Carbohydr. Polym.* **2010**, *81*, 919.
18. Heath, L.; Zhu, L.; Thielemans, W. *ChemSusChem* **2013**, *6*, 537.
19. Tzoumaki, M. V.; Moschakis, T.; Biliaderis, C. G. *Biomacromolecules* **2010**, *11*, 175.
20. Marcilla, R.; Blázquez, J. A.; Fernandez, R.; Grande, H.; Pomposo, J. A.; Mecerreyes, D. *Macromol. Chem. Phys.* **2005**, *206*, 299.

21. Yuan, J.; Antonietti, M. *Polymer* **2011**, *52*, 1469.
22. Carrasco, P. M.; Ruiz de Luzuriaga, A.; Constantinou, M.; Georgopanos, P.; Rangou, S.; Avgeropoulos, A.; Zafeiropoulos, N. E.; Grande, H.-J.; Cabañero, G.; Mecerreyes, D.; Garcia, I. *Macromolecules* **2011**, *44*, 4936.
23. Katsigiannopoulos, D.; Grana, E.; Avgeropoulos, A.; Carrasco, P. M.; Garcia, I.; Odriozola, I.; Diamanti, E.; Gournis, D. *J. Polym. Sci. Part A: Polym. Chem.* **2012**, *50*, 1181.
24. Kvien, I.; Tanem, B. S.; Oksman, K. *Biomacromolecules* **2005**, *6*, 3160.
25. Pretsch, E.; Bühlmann, P.; Affolter, C; Herrera, A.; Martinez, R. *Determinación Estructural de Compuestos Orgánicos*; Springer-Verlab Iberica: Barcelona (Spain), **2001**; Chapter *6*, p 245.
26. Dharaskar, S. A.; Varma, M. N.; Shende, D. Z.; Yoo, C. Y.; Wasewar, K. L. *Sci. World J.* **2013**, *2013*, 395274.
27. Sardon, H.; Irusta, L.; Fernandez-Berridi, M. *J. Prog. Org. Coat.* **2009**, *66*, 291.
28. Rueda, L.; Fernandez d'Arlas, B.; Zhou, Q.; Berglund, L. A.; Corcuera, M. A.; Mondragon, I.; Eceiza, A. *Compos. Sci. Technol.* **2011**, *71*, 1953.
29. Cárdenas, G.; Cabrera, G.; Taboada, E.; Miranda, S. P. *J. Appl. Polym. Sci.* **2004**, *93*, 1876.
30. Hasani, M.; Cranston, E. D.; Westmana, G.; Gray, D. G. *Soft Matter* **2008**, *4*, 2238.
31. Giesche, H. Mercury Porosimetry: A General (Practical) Overview, Particle and Particle Systems Characterization; Wiley: New York, **2006**; Vol. *23*, p 9.